This article was downloaded by:
On: *21 January 2011*
Access details: *Access Details: Free Access*
Publisher *Taylor & Francis*
Informa Ltd Registered in England and Wales Registered Number: 1072954 Registered office: Mortimer House, 37-41 Mortimer Street, London W1T 3JH, UK

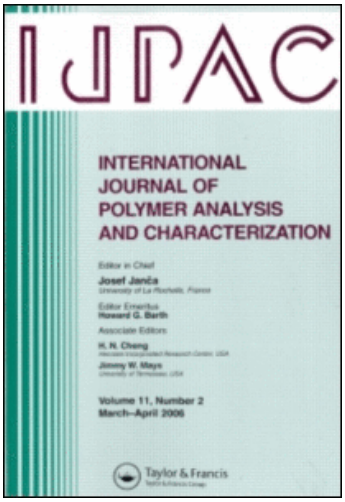

International Journal of Polymer Analysis and Characterization
Publication details, including instructions for authors and subscription information:
http://www.informaworld.com/smpp/title~content=t713646643

Straight-Chain Segment Length Distributions in UHMWPE Reactor Powders of Different Morphological Types

V. Galitsyn[a]; S. Gribanov[a]; M. Kakiage[b]; H. Uehara[b]; Svetlana Khizhnyak[c]; P. Pakhomov[c]; Eleonora Moeller[d]; V. Nikitin[e]; V. Zakharov[e]; A. Tshmel[f]
[a] Institute of Synthetic Fiber, Tver', Russia [b] Department of Chemistry, Gunma University, Kiryu, Gunma, Japan [c] Physico-Chemistry Department, Tver' State University, Tver', Russia [d] University Osnabrüeck, Osnabrüeck, Germany [e] Boreskov Institute of Catalysis, Siberian Division of Russian Academy of Sciences, Novosibirsk, Russia [f] Ioffe Physico-Technical Institute, Russian Academy of Sciences, St. Petersburg, Russia

To cite this Article Galitsyn, V. , Gribanov, S. , Kakiage, M. , Uehara, H. , Khizhnyak, Svetlana , Pakhomov, P. , Moeller, Eleonora , Nikitin, V. , Zakharov, V. and Tshmel, A.(2007) 'Straight-Chain Segment Length Distributions in UHMWPE Reactor Powders of Different Morphological Types', International Journal of Polymer Analysis and Characterization, 12: 3, 221 — 230
To link to this Article: DOI: 10.1080/10236660701245264
URL: http://dx.doi.org/10.1080/10236660701245264

PLEASE SCROLL DOWN FOR ARTICLE

Full terms and conditions of use: http://www.informaworld.com/terms-and-conditions-of-access.pdf

This article may be used for research, teaching and private study purposes. Any substantial or systematic reproduction, re-distribution, re-selling, loan or sub-licensing, systematic supply or distribution in any form to anyone is expressly forbidden.

The publisher does not give any warranty express or implied or make any representation that the contents will be complete or accurate or up to date. The accuracy of any instructions, formulae and drug doses should be independently verified with primary sources. The publisher shall not be liable for any loss, actions, claims, proceedings, demand or costs or damages whatsoever or howsoever caused arising directly or indirectly in connection with or arising out of the use of this material.

International Journal of Polymer Anal. Charact., 12: 221–230, 2007
Copyright © Taylor & Francis Group, LLC
ISSN: 1023-666X print
DOI: 10.1080/10236660701245264

Taylor & Francis
Taylor & Francis Group

Straight-Chain Segment Length Distributions in UHMWPE Reactor Powders of Different Morphological Types

V. Galitsyn and S. Gribanov
Institute of Synthetic Fiber, Tver', Russia

M. Kakiage and H. Uehara
Department of Chemistry, Gunma University, Kiryu, Gunma, Japan

Svetlana Khizhnyak and P. Pakhomov
Physico-Chemistry Department, Tver' State University, Tver', Russia

Eleonora Moeller
University Osnabrüeck, Osnabrüeck, Germany

V. Nikitin and V. Zakharov
Boreskov Institute of Catalysis, Siberian Division of Russian Academy of Sciences, Novosibirsk, Russia

A. Tshmel
Ioffe Physico-Technical Institute, Russian Academy of Sciences, St. Petersburg, Russia

Downloaded At: 15:56 21 January 2011

Abstract: A series of reactor powders of ultrahigh molecular weight polyethylene obtained using supported and unsupported Ziegler catalysts were studied with the help of low-frequency Raman spectroscopy. This experimental technique allows

This work was supported by DAAD (Germany) and RFBR (Russia), grants no. 06-03-32609a and 06-03-08111 ofi.

Address correspondence to Alexandre Tshmel, Ioffe Physico-Technical Institute, Russian Academy of Sciences, 26 Polytekhnicheskaya, 194021 St. Petersburg, Russia. E-mail: alex@ac7773.spb.edu

one to calculate the length distribution of straight-chain segments (SCS) in a polymer sample without differing between the SCS localized in either crystalline or amorphous regions of the sample. A comparison of the scanning electron microscopy images of powders with their SCS distributions showed that the samples with pronounced fibrous morphology exhibit bimodal distribution functions, while the granular morphological pattern yields unimodal SCS length distributions.

Keywords: Low-frequency Raman spectroscopy; Polyethylene; Reactor powder

Downloaded At: 15:56 21 January 2011

INTRODUCTION

A diversity of morphological structures of polyethylene reactor powders with different synthesis histories has stimulated researchers to establish a correlation between the morphology of a given powder and particular properties of the technologically remote products obtained from it.[1–3] A case in point is the performance of highly drawn fibers or films, including their draw ratio (DR), tensile strength, and Young's modulus. The problem is particularly complicated when powders of similar morphology are subjected to different technological procedures, such as submelt compactization,[1,2] melt crystallization,[3] or gel technology.[4]

The forecast of the performance of the final product issuing from the morphology of the original material could be more grounded if one establishes the molecular characteristics of the main features of the morphological pattern inherent to powders: globules, linking fibrils, individual fibrils, etc. In the sequence of treatments that a reactor powder undergoes when transforming to a highly drawn fiber, the initial morphology disappears completely, while the remnant features of the primary molecular structure manifest themselves at various stages of fiber manufacturing.[3–5] In this work, a collection of reactor powders of ultrahigh molecular weight polyethylene (UHMWPE) with different particle shapes (globular, fibrous, or complex) was studied. The powders were specified by their straight-chain segment (SCS) length distributions, that is, by the characteristics of the ensemble of all-trans sequences typical for each sample. The measurements were carried out with the help of low-frequency Raman spectroscopy, which had earlier been successfully used for characterization of reactor powders with different molecular weight (MW) and MW distributions.[4,5]

EXPERIMENTAL SECTION

Two sets of reactor powders (four samples in each set) originating from Russian (samples A–D) and Japanese (samples E–H) manufacturers were used in the experiments. The scanning electron microscope (SEM) images of the powders synthesized using two catalytic systems are shown in

Figures 1 and 2. Samples A–D were prepared using supported $TiCl_4/MgCl_2$ catalyst; the difference in their morphology (Figure 1) was achieved by varying both the temperature of polymerization (T_{poly}) and the technology of production of the supporting substance. Samples E–H were obtained with the help of unsupported, highly active Ziegler catalyst; in this case, a significant difference in the morphological pattern of synthesized powders was induced by applying different T_{poly} (Figure 2).

The basic characteristics of the investigated UHMWPE reactor powders were obtained from viscosity and differential scanning calorimetry (DSC) measurements (Table I). The DSC experiments were performed on a Seiko Instrument DSC-10. The scans were made from 80° to 180°C at a heating rate of 3°C/min under a N_2 gas flow. These DSC characteristics were calibrated by indium and tin standards.

The Raman studies were performed on a triple monochromator, Spex Model 1401, in the frequency range 5 to 40 cm^{-1}, where the longitudinal acoustic modes (LAM) localized on straight-chain segments of polymer macromolecules yield a specific peak.

Downloaded At: 15:56 21 January 2011

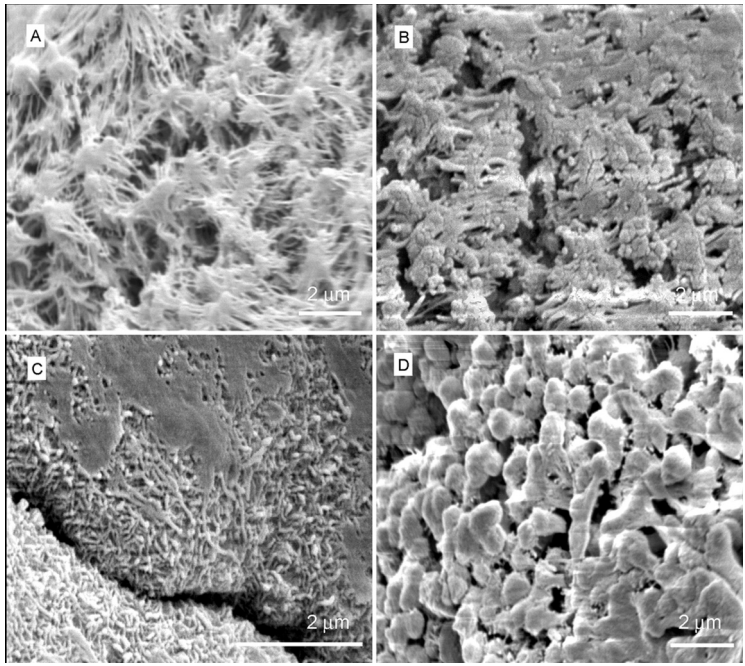

Figure 1. SEM images of powders synthesized using supported $TiCl_4/MgCl_2$ catalyst. In all figures, the lettering denotes samples characterized in Table I.

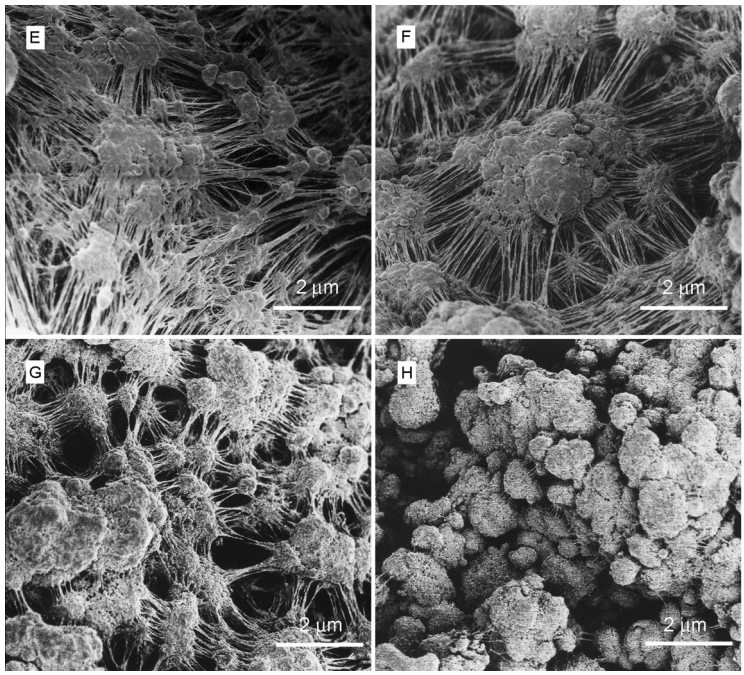

Figure 2. SEM images of powders synthesized using unsupported Ziegler catalyst.

Downloaded At: 15:56 21 January 2011

Table I. Characteristics of UHMWPE reactor powders

Sample	Catalyst	Morphology	T_{poly}, °C	10^{-6} MW[a]	T_m[b], °C	Crystallinity[c], %
A	Supported	Cob-web fibrous	55	3.4	141.7	68
B		Semi-open fibrous	60	2.0	140.6	64
C		Compacted small fibrous	60	2.5	140.1	62
D		Open granular	70	2.4	140.9	63
E	Unsupported	Cob-web organization with different relative contribution of globules and fibrils	90	1.7	140.5	67
F			80	1.9	140.6	68
G			60	2.2	140.8	67
H			20	2.0	140.0	65

[a]Viscosity-average molecular weight.
[b]From DSC first run.
[c]From DSC heats of fusion.

The LAM band in the low-frequency Raman spectrum allows one to find the SCS length distribution in a PE sample. It is important that the localization of the SCS in crystalline or amorphous regions is not counted, since the acoustic vibrations of this kind are excited in individual macromolecules and have a very low sensitivity to the nature of the chain environment.

Length of the ordered (all-*trans*) sequence, L, and LAM frequency, ω_L, are related by:

$$L = (2c\omega_L)^{-1} \times \left(\frac{E}{\rho}\right)^{1/2} \quad (1)$$

where c is the speed of light, ρ is density, and E is the chain Young's modulus.

As far as each *all-trans* stem of a given length has its specific LAM frequency, the LAM band in whole reflects the contribution of SCS of different lengths to the Raman intensity. However, owing to the dependence of distribution function F(L) not only upon the number of vibrating SCS but also upon the scattering efficiency of light and the population of vibrational energy levels, the original Raman spectrum is poorly representative for quantitative estimations, and F(L) must be calculated using a routine procedure based on the relationship:[6]

$$F(L) \propto \left[1 - \exp\left(\frac{-hc\omega}{kT}\right)\right]\omega^2 I \quad (2)$$

Here, h is the Planck constant, k is the Boltzmann constant, T is the absolute temperature, and I is Raman intensity. The expression in brackets characterizes the Boltzmann population of vibrational energy levels. The value of distribution function at given L is proportional to the fraction amount of the SCS with length equal to L.

In view of a very high level of parasitic light scattering from the powders in the low-frequency spectral range, all samples were scanned six times with subsequent averaging of the data and subtracting the background. In addition, relationship (2) does not take into account the fact that the Raman signal in the vicinity of the central line is a sum of the Rayleigh component and the LAM band intensity. To exclude the former contribution, a portion of central line under the LAM spectrum could be approximated with an appropriate function. The Lorentz function was used in this study. Data points were selected at the periphery of the measured frequency range where the LAM band intensity could be regarded as negligible. The difference between the experimental spectrum averaged over six scans and the approximating Lorentzian was taken as the effective intensity I in Equation (2).

Downloaded At: 15:56 21 January 2011

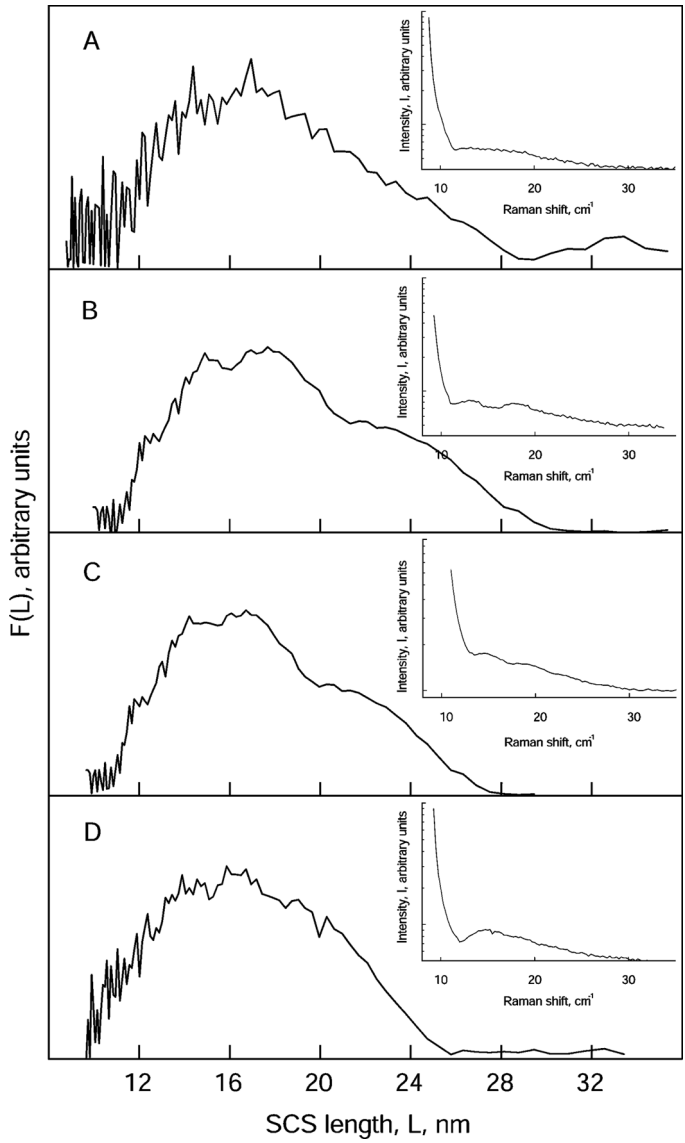

Figure 3. Raman spectra of the reactor powders synthesized using supported $TiCl_4/MgCl_2$ catalyst (inset) and the SCS length distributions calculated from relevant spectra.

Downloaded At: 15:56 21 January 2011

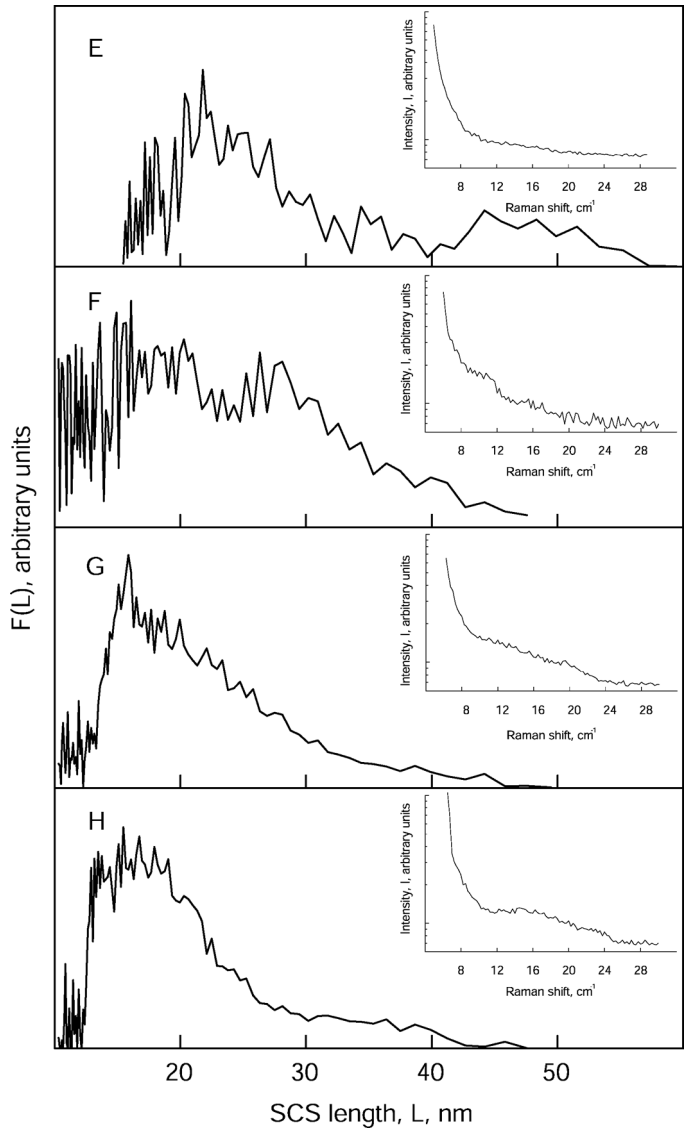

Figure 4. Raman spectra of the reactor powders synthesized using unsupported Ziegler catalyst and the SCS length distributions calculated from relevant spectra.

RESULTS

According to the SEM images, both series contain samples with typical cob-web organization (A, Figure 1, and E, Figure 2) and those

Downloaded At: 15:56 21 January 2011

with granular organization (D, Figure 1, and H, Figure 2). Other powders exhibit more complicated intermediate or complex patterns.

The low-frequency Raman spectra and the calculated SCS length distributions are shown in Figures 3 and 4 for series A–D and E–H, respectively. The distribution functions for all samples in both series exhibit main peaks at ~16 nm (with the exception of sample E, where the main peak position is about 22 nm), which in samples A–C and E–G are accompanied with smaller peaks or shoulders. A comparison of the SEM images with the SCS length distributions reveals well-resolved bimodal functions F(L) for the samples with pronounced cob-web structure (A and E) and unimodal distributions for granular powders (D and H). The overlapping peaks in the SCS length distributions in other samples reflect the relative contribution of varying length all-trans sequences situated in grains and fibrils of the structural framework.

The length of the most extended SCS reaches 30 nm in the samples obtained with a supported catalyst and ~50 nm in the samples polymerized with an unsupported catalyst.

Downloaded At: 15:56 21 January 2011

DISCUSSION

A relatively low melting point (T_m = 140–141°C) in combination with symmetrically shaped main peaks of the F(L) function implies the presence of folded chain crystals (FCC) in all samples. (In the case of extended chain crystals, which are specified by the transversal order and longitudinal length diversity, one should expect a higher T_m and a broader SCS length distribution.) A previous transmission electron microscope study of different reactor powders[7] evidenced the presence of a population of stacked folded crystals in globular elements. We suppose that the revealed unimodal SCS length distributions in our granular samples confirm this finding. The structure of fibrous powders is more complicated and contains both lamellar and "bundle-like" crystals. Interestingly, in both series of our samples manufactured under quite different conditions, the dimension of suggested folds was approximately the same (16 nm). The shifted position of the main maximum in sample H (at 22 nm) can be explained by the very high temperature of its polymerization (90°C). A significant heat extension during synthesis forced partial unfolding of lamellar chains in a manner similar to the necking effect when drawing the films. The integral SCS distribution reflects the complicated structure of the disturbed grains and highly extended fibrils.

Smaller peaks of the longest SCS are highly sensitive to details of the powder preparation procedure and, therefore, cannot be referred to the FCC. These additional long-length peaks in the SCS distributions

manifest themselves only in powders with developed fibrillar structure, and their positions are shifted to longer L in the samples with more extended fibrils. Thus, we conclude that in granular powders, the FCC structure prevails, while the fibrous elements consist of individual or bundled long all-trans sequences.

The shown interconnection between the morphology of reactor powders and their molecular structure is of importance in the light of the previously established correlation between the imaged aspect of powder particles and the performance of fibers manufactured from these powders.[1–3] The data obtained in this work provide insight into the nanoscopic organization of the elements composing the morphological pattern of powders, thus establishing a structural correlation between the microscopic and molecular scale levels. The presence of long (up to 50 nm) SCS in fibrous particles indicates the existence of rigid stems that hinder the submelt treatment of the material, including the compacting procedure.

To summarize, the UHMWPE reactor powders manufactured under different synthesis conditions represent a variety of morphological structures whose main elements are globules and fibrils. Low-frequency Raman study demonstrates that a hallmark of the predominant cobweb structure (globules linked by fibrils) is the bimodal SCS length distribution: the SCS ensemble includes both the FCC 15 to 20 nm in length situated in globules and bundles of non-folded SCS whose length reaches 50 nm. The predominant globular morphology is characterized by the unimodal SCS length distribution typical for FCC-composed structures. Diverse intermediate situations occurring in the morphology of powders are reflected adequately in the SCS length distributions.

Downloaded At: 15:56 21 January 2011

REFERENCES

[1] Truss, R. W., K. S. Han, J. F. Wallace, and P. H. Geil. (1980). Cold compaction molding and sintering of ultra high molecular weight polyethylene. *Polym. Eng. Sci.* **20**, 747–754.

[2] Han, K. S., J. F. Wallace, R. W. Truss, and P. H. Geil. (1981). Powder compaction, sintering and rolling of ultra high molecular weight polyethylene and its composites. *J. Macromol. Sci. Phys.* **B19**, 313–349.

[3] Ivan'kova, E. M., L. P. Myasnikova, V. A. Marikhin, A. A. Baulin, and B. Z. Volchek. (2001). On the memory effect in UHMWPE nascent powders. *J. Macromol. Sci. Phys.* **B40**, 813–832.

[4] Tsobkallo, K., V. Vasilieva, S. Khizhnyak, P. Pakhomov, V. Galitsyn., E. Ruhl, V. Egorov, and A. Tshmel. (2004). *Polymer* **43**, 1613–1618.

[5] Tsobkallo, K., V. Vasilieva, M. Kakiage, H. Uehara, and A. Tshmel. (2006). *J Macromol. Sci. Phys.* **B45**, 407–415.

[6] Capaccio, G., M. A. Wilding, and I. M. Ward. (1981). Morphology of high-modulus polyethylene:A study by Raman spectroscopy. *J. Polym. Sci. Polym. Phys. Ed.* **19**, 1489–1496.
[7] Uehara, H., T. Aoike, T. Yamanobe, and T. Komoto. (2002). Solid-state ^{1}H NMR relaxation analysis of ultrahigh molecular weight polyethylene reactor powder. *Macromolecules* **35**, 2640–2647.

Downloaded At: 15:56 21 January 2011